Int J Adv Manuf Technol (2017) 92:3311–3318
DOI 10.1007/s00170-017-0401-3

ORIGINAL ARTICLE

Experimental investigation of friction in deep drawing

Hakan Kalkan[1] · **Tugce Hacaloglu**[2] · **Bilgin Kaftanoglu**[2]

Received: 11 October 2016 / Accepted: 3 April 2017 / Published online: 21 April 2017

Abstract Investigation of friction is carried out in the radial drawing region between the die and blank holder and also in the stretching zone over the punch in deep drawing. Two methods are developed to calculate the coefficient of friction in each zone using the experimentally determined data such as punch force diagrams and strain distributions obtained by an optical scanning system. The current methods differ from the existing techniques which are obtained in simulative tests. The proposed methods can be applied in room temperature and at elevated temperatures. Comparisons of friction coefficients are made with those obtained by other techniques.

Keywords Friction · Deep drawing · Tribology

1 Introduction

Friction is an important process parameter which controls the flow of material in the tool and the final quality of produced parts. It is important to know the magnitude of friction for a number of reasons. Estimation of load, energy requirements, tool wear of a deformation process can only be made with the knowledge of friction. In order to accurately predict the final shape or to design a deformation process to produce a given shape and find the loads applied to the workpiece, a thorough knowledge of friction is necessary.

The development of the finite element (FE) method for analysis of plastic deformation processes has provided a powerful tool for process simulation and optimization, which is a great value especially in the case of designing tools for sheet metal forming operations. To obtain reliable predictions of flow, strains, and stresses, it is vital to have a reliable friction model. An accurate forming analysis can be done if the material behavior and friction conditions are modeled accurately. For material models, significant improvements have been made over the recent decades but majority of the simulations still use approximations for friction coefficients.

The aim of this study is to improve the efficiency of sheet metal forming processes by using new methods to evaluate friction by using the experimental data such as strain distributions and punch load curves in the deep drawing process. Surface roughness, nanohardness of thin film coatings, and scratch tests for adherence of coatings can also help to identify the surface characterization. Effects of lubrication and temperature can also be investigated using the proposed techniques.

Previous research about investigation of friction in sheet metal forming provided the basis of the current study but the calculation of friction coefficient due to nonlinear extrapolation and the manual measurement of strains resulted in higher errors [1]. It was also limited to room temperature.

In the past studies, strip draw and deep draw tests were commonly used to evaluate the stamping lubricants. In such research, water-based lubricants performed better than petroleum-based lubricants and also coefficient of friction reduced with the increase in blankholder force with all other conditions remaining unchanged [3]. Many studies

✉ Hakan Kalkan
hakan.kalkan@atilim.edu.tr

[1] Manufacturing Engineering Department, ATILIM University, Ankara, Turkey

[2] Metal Forming Center of Excellence, ATILIM University, Ankara, Turkey

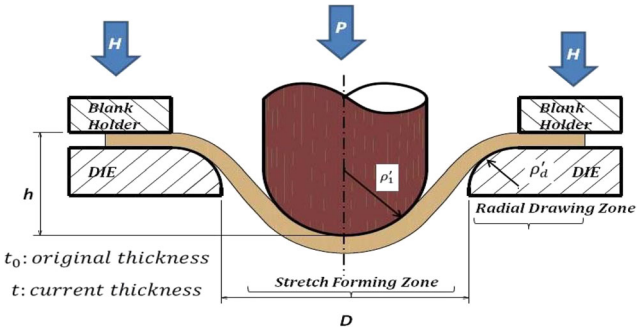

Fig. 1 Main features of deep drawing

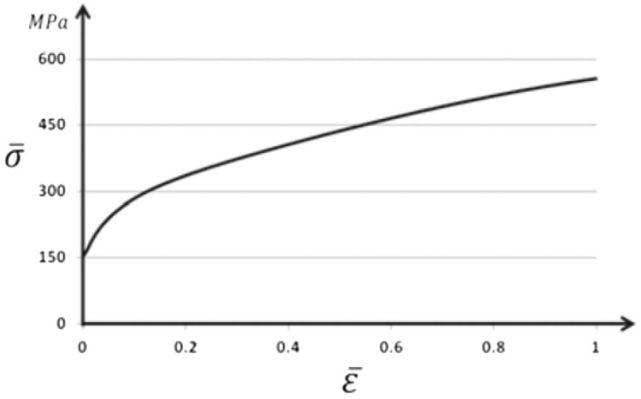

Fig. 3 Flow curve of the EN10346/DX54D+Z steel

have been focused on explaining friction mechanisms under different loading conditions in forming operations using experimental, analytical, and numerical methods. Although some basic friction characterization is obtained at present, friction mechanism still is not properly understood in depth since it is a highly complex process. The main contribution of this study is to develop new techniques to calculate the friction coefficient to get more accurate results for the finite element simulations. This will reduce the cost and the operation time in sheet metal forming.

The coefficient of friction under lubricated conditions at elevated temperature was also found. It was shown that the use of lubricants was effective for decreasing the stamping load and die wear in hot stamping [4]. Coefficient of friction data obtained in strip drawing test was used in another study to show the importance of the lubrication on process parameters [5].

The drawibility and frictional characteristics of pure molybdenum sheet at elevated temperature were investigated, and inverse comparison method was used to evaluate the frictional conditions [6]. Effect of die radius, surface roughness of the tools, drawing speed, blank holder force, and lubrication type on coefficient of friction between flange and radius regions of the tools and sheet metal was investigated [7].

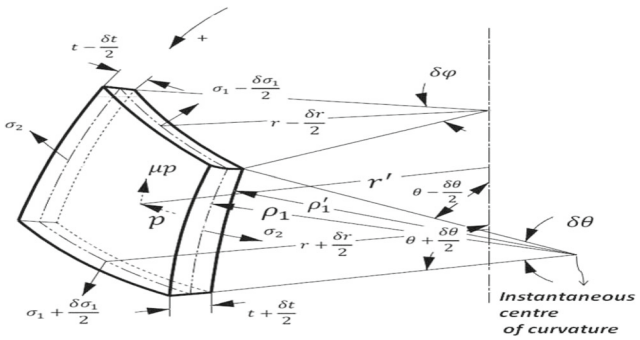

Fig. 2 Stresses on element of shell wall

Surface parameters also affect the coefficient of friction. Research was conducted to investigate this effect. Deformation of sheet metal during forming was investigated and surface parameters were derived from three-dimensional surface measurements [8]. Correlation between the surface topography of dies and friction with sheet were investigated in another study and correlation between friction and texture characterization parameters were observed [9]. Friction forces modeled by introducing a relation between the surface parameters [10].

Results from such simulative tests were used in finite element analysis as input. Such simulations are important tools for sheet metal forming industry and importance of the friction data were emphasized [12]. Based on recent advances in friction modeling, a pressure slip rate and temperature-dependent friction model suited for numerically stable multi-dimensional regression analysis was presented and implemented in Abaqus [11].

2 Theory

2.1 Method 1: deep drawing

Radial drawing zone can be seen in Fig. 1. There is friction between sheet metal, die, and blankholder. For radial drawing region, an expression can be derived by using the vertical and horizontal equilibrium equations [1].

Coefficient of friction in radial drawing region can be calculated by using the following equation [2].

$$\mu = \frac{\delta P \cot\alpha}{2\delta H + 2\delta P} \tag{1}$$

From the geometry of Fig. 1, relationship between the bulge depth and α can be derived [2].

$$h = (\frac{D}{2} + \rho_d')\tan\alpha - (\rho_1' + \rho_d' + t_0)(\sec\alpha - 1) \tag{2}$$

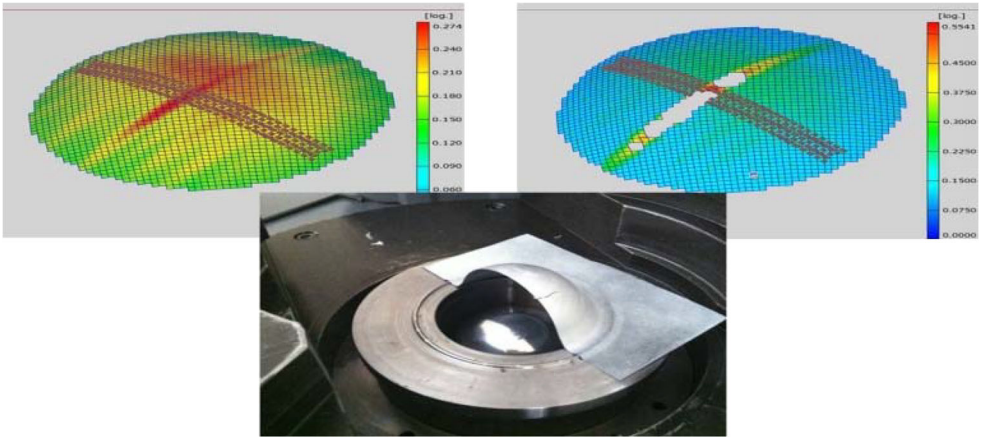

Fig. 4 Views from optical scanning system measurements

where
h : bulge depth
H : Blankholder load
P : Punch load
α : angle of embrace of the die
ρ_d' : die radius
ρ_1' : meridional radius of curvature to inner shell wall

With two deep drawing tests under identical conditions, with only changing blank holder loads, it is possible to calculate coefficient of friction using the incremental punch loads in Eq. 1. This technique can be used at room temperature or at high temperatures provided that the appropriate data is obtained.

2.2 Method 2: stretch forming

In the stretch forming zone, coefficient of friction can also be calculated by using the equilibrium and the plasticity equations. Figure 2 shows the stresses acting on an element of shell wall.
where
h : bulge depth
p : interfacial pressure between punch and sheet metal
k : stress ratio= $\dfrac{\sigma_3}{\sigma_1}$

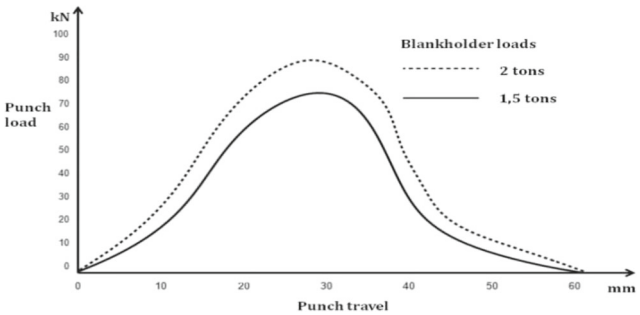

Fig. 5 Punch loads at different blank holder loads for EN 10268 steel

x : stress ratio= $\dfrac{\sigma_2}{\sigma_1}$
r_0 :original radius to mean shell wall
r :current radius to mean shell wall
$\epsilon_1, \epsilon_2, \epsilon_3$:true plastic strains in meridional, circumferential and thickness directions.
θ : angle, that normal to an element of shell wall makes with the vertical
μ : coefficient of friction
ρ_1 : meridional radius of curvature to mean shell wall
Equilibrium equation in radial direction is [1]

$$\frac{1}{r}\frac{d}{dr}(\sigma_1 tr)+\left[p\rho_1'\frac{r'}{r}(\tan\theta-\mu)-t\sigma_1\tan\theta-\sigma_2\frac{\rho_1 t}{r\cos\theta}\right]\frac{d\theta}{dr}=0 \tag{3}$$

In vertical direction [1]

$$\frac{1}{r}\frac{d}{dr}(\sigma_1 tr)+\left[\sigma_1 t\cot\theta-p\rho_1'\frac{r'}{r}(\cot\theta+\mu)\right]\frac{d\theta}{dr}=0 \tag{4}$$

Subtracting Eq. 4 from Eq. 3

$$p=\frac{t}{\rho r}(\sigma_1 r+\sigma_2\rho_1\sin\theta) \tag{5}$$

From Eq. 5, it is clear that the interfacial pressure is a function of θ. In addition to θ angle, σ_1 and σ_2 stresses must be known to calculate the pressure, but it is not possible to measure the stresses during the deformation. These two

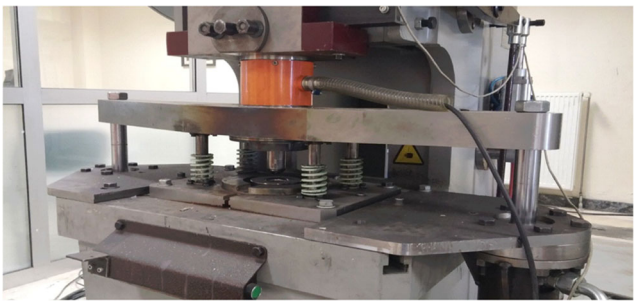

Fig. 6 Deep drawing test apparatus

Table 1 Coefficient of friction values from method 1 (for the radial drawing region)

Material grade	Lubricant	Angle	Blankholder loads (N)	Coefficient of friction	
				Room temp.	(300 °C)
EN 10268	Dry	15		0.381	0.303
		30	22350	0.325	0.236
		35	14900	0.281	0.202
		40		0.245	0.204
EN 10268	Dry	15		0.359	0.357
		30	29800	0.339	0.357
		35	22350	0.322	0.297
		40		0.304	0.291
EN 10268	Graphite	15		0.117	0.174
		30	22350	0.094	0.133
		35	14900	0.083	0.149
		40		0.074	0.135
EN 10268	Graphite	15		0.153	0.151
		30	29800	0.100	0.206
		35	22350	0.131	0.155
		40		0.070	0.138

stresses can be calculated approximately, by using the strain distributions and the flow curve of the material.

Then, effective strain can be calculated with the following equation for isotropic materials:

$$\overline{\epsilon} = \sqrt{\frac{2}{3}\left(\epsilon_1^2 + \epsilon_2^2 + \epsilon_3^2\right)} \tag{6}$$

For the corresponding values, effective stresses can be obtained from the stress strain curve shown in Fig. 3.

Strain distributions on the stretch forming zone of the workpiece can be measured by using an optical scanning system as shown in Fig. 4 at different stages.

Assuming

$$\frac{\sigma_3}{\sigma_1} \cong 0 \tag{7}$$

Effective stress will be equal to

$$\overline{\sigma} = \sqrt{\left(\sigma_1^2 - \sigma_1\sigma_2 + \sigma_2^2\right)} \tag{8}$$

Relation between the σ_1 and σ_2 values can be obtained from the strain measurements.

$$\frac{d\epsilon_1}{d\epsilon_2} = \frac{\frac{2}{3}d\lambda[\sigma_1 - \frac{1}{2}(\sigma_2 + \sigma_3)]}{\frac{2}{3}d\lambda[\sigma_2 - \frac{1}{2}(\sigma_1 + \sigma_3)]} = r_\varepsilon \tag{9}$$

$$\frac{\sigma_2}{\sigma_1} = \frac{2r_\epsilon + 1}{2 + r_\epsilon} \tag{10}$$

Interfacial pressure can be calculated by the following equation:

$$p = \sigma_1 t\left[\frac{1}{\rho} + \frac{x\sin\theta}{r}\right] \tag{11}$$

Recalling the Eqs. 3 and 4 in vertical and radial directions,

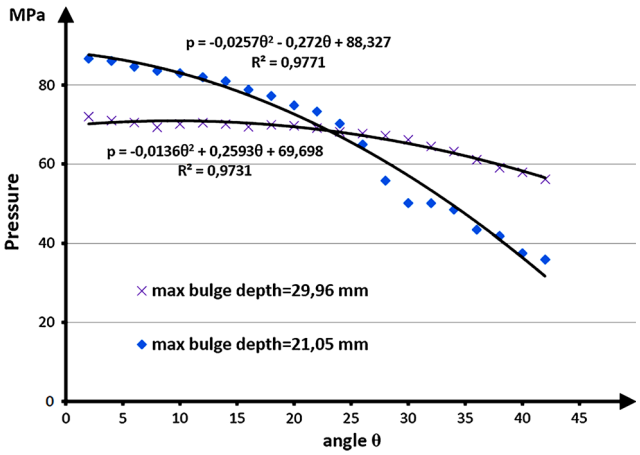

Fig. 7 EN 10346/HX220BD+Z steel interfacial pressure distributions

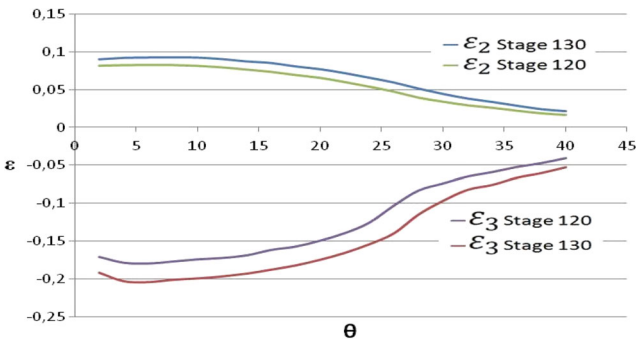

Fig. 8 EN 10346/HX220BD+Z steel strain distributions

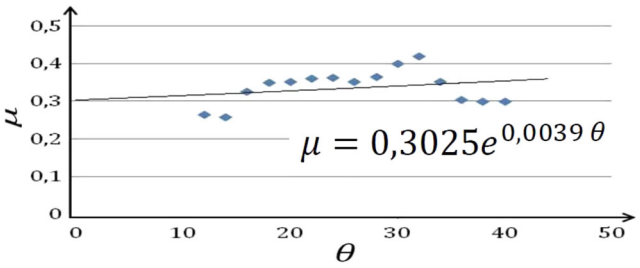

Fig. 9 Coefficient of friction values for EN 10346/HX220BD+Z using Eq. 32

For a hemispherical punch

$$r = \rho_1 \sin\theta \text{ and } dr = \rho_1 \cos\theta d\theta \tag{12}$$

and for thin shells

$$r = r' \text{ and } \rho_1 = \rho_1' \tag{13}$$

Substituting Eqs. 12 and 13 in Eq. 4

$$\frac{d\sigma_1}{d\theta} + 2\sigma_1 t \cot\theta = p\rho\,(\cot\theta + \mu) \tag{14}$$

Equation 14 is a first order linear differential equation. To solve this equation, each term is multiplied by $e^{\int 2\cot\theta d\theta}$

$$(\sigma_1 t)'(\sin\theta)^2 + 2(\sigma_1 t)\cot\theta(\sin\theta)^2 = p\rho(\cot\theta + \mu)(\sin\theta)^2 \tag{15}$$

$$(\sigma_1 t)'(\sin\theta)^2 + 2(\sigma_1 t)\frac{\cos\theta}{\sin\theta}(\sin\theta)^2 = p\rho(\frac{\cos\theta}{\sin\theta} + \mu)(\sin\theta)^2 \tag{16}$$

$$(\sigma_1 t)'(\sin\theta)^2 + 2(\sigma_1 t)\sin\theta\cos\theta = p\rho\sin\theta\cos\theta + p\rho\mu(\sin\theta)^2 \tag{17}$$

$$(\sigma_1 t)'(\sin\theta)^2 + (\sigma_1 t)\sin 2\theta = p\rho\sin\theta\cos\theta + p\rho\mu(\sin\theta)^2 \tag{18}$$

$v'u + u'v + = (uv)'$
$(uv)' = p\rho\sin\theta\cos\theta + p\rho\mu(\sin\theta)^2$
here $u = (\sin\theta)^2$ so, $v = (\sigma_1 t)$

$$(\sigma_1 t(\sin\theta)^2)' = p\rho\sin\theta\cos\theta + p\rho\mu(\sin\theta)^2 \tag{19}$$

$$\sigma_1 t(\sin\theta)^2 = \int p\rho\sin\theta\cos\theta d\theta + \int p\rho\mu(\sin\theta)^2 d\theta \tag{20}$$

$$\sigma_1 t(\sin\theta)^2 = \rho\int p\sin\theta\cos\theta d\theta + \rho\mu\int p(\sin\theta)^2 d\theta \tag{21}$$

By using Eq. 11, interfacial pressure can be expressed as

$$p = a\theta^2 + b\theta + c \tag{22}$$

$$\begin{aligned}\int p\sin\theta\cos\theta d\theta = \frac{1}{8}[&(-4c(\cos\theta)^2)\\ &+(a - 2b\theta - 2a\theta^2)\cos(2\theta)\\ &+(b + 2a\theta)\sin(2\theta)]\end{aligned} \tag{23}$$

$$\begin{aligned}\int p(\sin\theta)^2 d\theta = &\frac{[2\theta(6c + 3b\theta + 2a\theta^2}{24}\\ &-\frac{3(b + 2a\theta)\cos(2\theta)}{24}\\ &-\frac{3(-a + 2c + 2b\theta + 2a\theta^2)\sin(2\theta)}{24}\end{aligned} \tag{24}$$

$$\sigma_1 t(\sin\theta)^2 = \rho A + \rho\mu B \tag{25}$$

$$\sigma_1 t(\sin\theta)^2 = \rho(A + \mu B) \tag{26}$$

Table 2 Coefficient of friction values obtained from method 2 (for stretch forming zone)

Test	Material grade	Lubricant	Bulge depths h (mm)	Coefficient of friction
1	EN 10346/DX54D+Z	Dry	21.50−19.08	0.294
2	EN 10346/DX54D+Z	Dry	29.96−25.13	0.338
3	EN 10346/HX380LAD+Z	Dry	17.11−14.73	0.251
4	EN 10346/HX380LAD+Z	Dry	21.85−19.47	0.320
5	EN 10346/ HX220BD+Z	Dry	20.61−18.25	0.302
6	EN 10346/HX220BD+Z	Dry	25.44−23.03	0.337
7	EN 10346/DX54D+Z	Paraffin	23.76−22.59	0.088
8	EN 10346/HX380LAD+Z	Paraffin	14.62−12.81	0.074
9	EN 10346/HX380LAD+Z	Paraffin	17.94−16.34	0.111

Table 3 Chemical Compositions of the steels used in the experiments

Chemical composition (%) Corresponding			C max.	Si max.	Mn max	P max	S max	Al max	V max	Nb max	Ti max
Standard	Similar standard	Erdemir Steel Grade									
EN 10268	–	7140	0.14	0.50	1.60	0.030	0.025	0.015	–	0.090	0.15
EN 10346/ HX220BD+Z	52814/9.52873	380(1)(2)	0.007–0.06	0.50	0.15–0.70	0.05–0.09	0.03	0.02–0.07	–	–	–
EN 10346/ HX380LAD+Z	52811/9.52873	368(3)	0.12	0.50	1.50	0.030	0.030	0.015 (min)	0.10	0.10	
EN 10346/ DX54D+Z	52806/9.52873	326	0.008	0.03	0.30	0.025	0.020	0.02 (min)		0.035	0.11

1) % Ni+%Cu+%Cr+%Mo.0.5, 2) % C+% P.0.16 3) % Nb+Ti+V.0.22

$$\sigma_1 = \frac{\rho}{t(\sin\theta)^2}(A + \mu B) \tag{27}$$

$$\sigma_2 = \frac{p\rho}{t} - \sigma_1 \tag{28}$$

$$\sigma_2 = \frac{p\rho}{t} - \frac{\rho}{t(\sin\theta)^2}(A + \mu B) \tag{29}$$

$$\sigma_2 = \frac{p}{t}[p - \frac{1}{t(\sin\theta)^2}(A + \mu B)] \tag{30}$$

$$\frac{\sigma_2}{\sigma_1} = \frac{p - \frac{1}{(\sin\theta)^2}(A + \mu B)}{\frac{1}{(\sin\theta)^2}(A + \mu B)} \tag{31}$$

To calculate the coefficient of friction in stretch forming following equation can be used.

$$\mu = \frac{p - \frac{A}{(\sin\theta)^2}(x+1)}{\frac{B}{(\sin\theta)^2}(x+1)} \tag{32}$$

where

$$A = \frac{1}{8}\left[\left(-4c(\cos\theta)^2\right) + \left(a - 2b\theta - 2a\theta^2\right)\cos 2\theta + (b + 2a\theta)\sin 2\theta\right]$$

$$B = \frac{1}{24}\left[2\theta\left(6c + 3b\theta + 2a\theta^2\right) - 3(b + 2a\theta)\cos 2\theta - 3\left(-a + 2c + 2b\theta + 2a\theta^2\right)\sin 2\theta\right]$$

3 Experiments

3.1 Method 1: deep drawing

In deep drawing tests, EN 10268 steel is used with dry and graphite lubrication. 1.5-mm thick sheet material and 42-mm-diameter hemispherical punch are used.

Two identical tests are performed at different blankholder loads and two different punch load curves are obtained as shown in Fig. 5.

Figure 6 shows the deep drawing press with the load cell and the data acquisition system. Blankholder/punch loads are used in the coefficient of friction calculations in Eq. 1, and the results are shown in Table 1.

3.2 Method 2: stretch forming

In stretch forming zone, nine different tests are carried out. Three different materials are used with dry and paraffin lubricated conditions. 1.2-mm thick, 250-mm square sheets are tested.

Using Eq. 11, interfacial pressure values can be calculated. Pressure distributions at two different stage values can be seen in Fig. 7.

Relation between the interfacial pressure and the angle $-\theta$ can be fitted to second order polynomial curve, Eq. 22. By using this relation in Eq. 32, interfacial pressure-dependent coefficient of friction values can be calculated.

As seen in Fig. 8, strain distributions are obtained from the optical scanning systems. Strain values are used in Eq. 32 and a typical result is shown in Fig. 9.

4 Results

4.1 Results obtained from method 1 (radial drawing zone) and method 2 (stretch forming zone)

In the radial drawing region, the surface roughness of the drawing die is found as R_a= 0.20 μm and the surface roughness of the sheet metal is around R_a= 1.82 μm as measured using an Alicona system.

Nine different stretch forming test results can be seen in Table 2. Coefficient of friction values are calculated

Table 4 Coefficient of friction values obtained by previous researchers

Type of test	Lubricant	Material	Coefficient of friction	Source
Bending tension	Oil	DP 600	0.14–0.16	[8]
Strip drawing	HBO 947/11 Mineral oil	AI99.5	0.15–0.32	[13]
Strip drawing	Mineral oil	A1100	0.2–0.23	[14]
Draw bead	Stamping oil	DP 600	0.12–0.16	[15]
Strip tension	Dry	AA 1050	0.29	[16]
Draw bead	Oil	AKDQ steel	0.08–0.17	[17]
Flat drawing	Dry	SPHC steel	0.45 (600 °C)	[18]
			0.45 (700 °C)	
			0.45 (800 °C)	
Hot stamping	Waterbase lubricant	SPHC steel	0.12 (600 °C)	[18]
			0.12 (700 °C)	
			0.12 (800 °C)	

by using strain distributions at two different stages. Bulge depths in Table 2 show the two stages of the test.

For the steel grades used in the experiments, chemical compositions are shown in Table 3.

4.2 Results obtained from other sources

Coefficient of friction values obtained from the previous researchers can be seen in Table 4. Room temperature and high temperature results can be seen to compare the test results with the previous studies.

5 Discussion

Coefficient of friction in deep drawing operations are investigated for two contact regions, i.e., radial drawing (method 1) and stretch forming zones (method 2). Previous studies as shown in Table 4, were performed using simulative test conditions such as strip drawing and bending under tension. However, this study was performed in a real deep drawing/stretch forming process.

Results obtained for the stretch forming tests as shown in Table 2 for dry conditions indicate a slight increase in coefficient of friction as a function of the bulge depth. It is seen that the use of paraffin as a lubricant is very effective and reduces the coefficient of friction drastically. If the strain data can be obtained at the higher temperatures, the method allows the calculation of coefficient of friction at such temperatures.

In the radial drawing region, for dry and graphite lubricated conditions at room temperatures, coefficient of friction slightly decreases as deformation progresses. This is a result of the flatting of the peaks during the process. Similar, but less pronounced behaviour is also observed at 300 °C. There is also a reduction in coefficient of friction at 300 °C under dry conditions. Graphite lubrication significantly lowers the coefficient of friction both in cold and hot conditions.

Coefficients of friction obtained in method 1 (radial drawing) and method 2 (stretch forming) regions fall in the same ranges. The values for coefficient of friction found in the literature fall in similar ranges with bigger variations as shown in Table 4. Since they are obtained in other simulative tests, such variations can be expected.

Results obtained from method 1 and method 2 can be used in finite element simulations to validate the efficiency of the results. Punch load curves and strain distributions can be used to compare the simulations and the test results.

6 Conclusion

Two methods are developed to evaluate coefficient of friction in radial drawing and stretch forming regions. The methods allow such evaluations also at high temperatures provided that the experimental data is available. Results obtained in dry and lubricated conditions agree with those found in the literature. It is seen that paraffin lubrication in stretch forming and graphite in radial drawing are very effective.

Acknowledgements This research was funded with the BAP Project at Atilim University. (ATU-BAP-A-1213-06).

The authors would like to thank the Metal Forming Center of Excellence (MFCE) and BOREN Center of Competence for Boron Coating at Atilim University, for the facilities used in the experiments.

References

1. Kaftanolu B (1973) Determination of coefficient of friction under conditions of deep-drawing and stretch forming. Wear 25/2:177–188

2. Kaftanoglu B, Alexander JM (1961) An Investigation of the Erichsen Test. J Inst Met 90:457–470
3. Subramonian S, Kardes N, Demiralp Y, Jurich M, Altan T (2011) Evaluation of stamping lubricants in forming galvannealed steels for industrial application. J Manuf Sci Eng 133/6:061001–9
4. Yanagida A, Azushima A (2009) Evaluation of coefficients of friction in hot stamping by hot flat drawing test. Ann CIRP 58/1:247–250
5. Bech J, Bay N, Eriksen M (1998) A study of mechanisms of liquid lubrication in metal forming. Ann CIRP 47/1:221–226
6. Meng B, Fu MW, Wan M (2014) Um sheet in deep-drawing process at elevated temperature. Int J Adv Manuf Technol 78:1005–1014
7. Dilmec M, Arap M (2016) Effect of geometrical and process parameters on coefficient of friction in deep drawing process at the flange and the radius regions. Int J Adv Manuf Technol 86:747–759
8. Schmoeckel D, Prier M, Staeves J (1997) Topography deformation of sheet metal during the forming process and its influence on friction. Ann CIRP 46/1:175–178
9. Berglund J, Brown CA, Rosén BG, Bay N (2010) Milled die steel surface roughness correlation with steel sheet friction. Ann CIRP 59/1:577–580
10. Jeon J, Bramley AN (2007) A friction model formicroforming. Int J Adv Manuf Technol 33:125–129
11. Klocke F, Trauth D, Shirobokov A, Mattfeld P (2015) FE-Analysis and in situ visualization of pressure-, slip-rate- and temperature-dependent coefficients of friction for advanced sheet metal forming: development of a novel coupled user subroutine for shell and continuum discretization, Int J Adv Manuf Technol 81:397–410
12. Makinouchi A, Teodosiu C, Nakagawa T (1998) Advance in FEM Simulation and its Related Technologies in Sheet Metal Forming. Ann CIRP 47/2:641–649
13. Vollertsen F, Hu Z (2006) Tribological size effects in sheet metal forming measured by a strip drawing test. Ann CIRP 55/1:291–294
14. Azushima A, Kudo H (1995) Direct observation of contact behaviour to interpret the pressure dependence of the coefficient of friction in sheet metal forming. Ann CIRP 44/1:209–212
15. Figueiredo L, Ramalho A, Oliveira MC, Menezes LF (2011) Experimental study of friction in sheet metal forming. Wear 271/910:1651–1657
16. Fratini L, Lo Casto S, Lo Valvo E (2006) A technical note on an experimental device to measure friction coefficient in sheet metal forming. J Mater Process Technol 172/1:16–21
17. Weinmann KJ, Kernosky SK (1996) Friction studies in sheet metal forming based on a unique die shoulder force transducer. Ann CIRP 45/1:269–272
18. Yanagida A, Azushima A (2009) Evaluation of coefficients of friction in hot stamping by hot flat drawing test. Ann CIRP 58/1:247–50